

2-dimensional OVFS Spreading for Chip-interleaved DS-CDMA Uplink Transmission

Le Liu[†] and Fumiyuki Adachi[‡]

Dept. of Electrical and Communication Engineering, Graduate School of Engineering,
Tohoku University, 6-6-05, Aza-Aoba, Aramaki, Aoba-ku Sendai 980-8580, JAPAN

[†]liule@mobile.ecei.tohoku.ac.jp, [‡]adachi@ecei.tohoku.ac.jp

Abstract—Multi-access interference (MAI) limits the transmission performance of the DS-CDMA uplink. In this paper, we propose 2-dimensional (2D)-OVFS spreading for chip-interleaved DS-CDMA uplink transmission. By adopting 2D-OVFS spreading, the multiuser channel is transformed into orthogonal single-user channels irrespective of users' data rates. Thus, single-user frequency-domain MMSE equalization can be used to take advantage of frequency-selective fading channel for signal detection. For a large Doppler spread, however, the orthogonality among the OVFS spreading codes may be lost, thereby producing the MAI. The decision feedback frequency-domain MAI cancellation is applied to improve the BER performance. The transmission performance in a multiuser and frequency- and time-selective fading environment is evaluated by computer simulation.

Key words: MAI, 2-dimensional, OVFS spreading codes, uplink, DS-CDMA.

1. INTRODUCTION

In multimedia wireless communications, a flexible support for the low-to-high bit rate of multimedia services upon a specific user's request is required [1]. Using code division multiple access (CDMA) technique [2], multi-rate services can be offered by changing the spreading factor (SF), the number of multiple codes, and/or modulation format (such as multi-level QAM (MQAM)) [3]. There may be two approaches in CDMA technique: direct sequence (DS)-CDMA [2], [4] and multicarrier (MC)-CDMA [5], [6]. With the aid of frequency-domain equalization (FDE), DS-CDMA can achieve good downlink performance similar to MC-CDMA while the former has an advantage of lower signal peak-to-average power ratio [7], [8]. However, in the uplink, different users' signals are asynchronous and go through different channels, resulting in multiple-access interference (MAI). The MAI is a critical performance limiting factor of the uplink.

A mutually orthogonal usercode-receiver (AMOUR) system [9] is proposed based on the orthogonal FDMA (OFDMA) principle [10], [11] for MAI-free multicarrier uplink transmission. Generalized MC-CDMA (GMC-CDMA) [12], [13] is the multi-rate AMOUR, which

preserves all the properties of AMOUR while being able to accommodate users of different data rates. For single-carrier DS-CDMA, chip-interleaving and time-domain spreading is proposed to cancel the MAI. Chip-interleaved DS-CDMA with guard interval (GI) [14], [15] can realize the MAI-free transmission in a quasi-synchronous multipath environment. The use of GI (i.e., zero-padding in [14] or cyclic prefix in [15]) not only avoids the inter-symbol interference (ISI) but also reduces the requirement for the synchronization. Frequency-domain equalization (FDE) instead of Rake combining is applied in a severe frequency-selective fading channel. The chip-interleaved DS-CDMA was considered in a single-cell environment [14], while Peng et al. extended to a multi-cell environment by using cell-specific scrambling codes [15]. The MUI-free transmission is guaranteed in a time-nonselective fading channel, where the block spreading maintains the code orthogonality among the spreading codes if the channel does not vary across the consecutive blocks.

In this paper, we propose 2-dimensional (2D)-OVFS spreading for chip-interleaved DS-CDMA uplink transmission. 2D-OVFS spreading can achieve a good BER performance, while accommodating users of different data rates under a quasi-synchronous multiuser environment (transmit timings of all users are only required to be kept within the GI). The combination of 2D-OVFS spreading and chip-interleaving makes it possible to get both the time- and frequency-domain diversity gains. The average BER performance of 2D-OVFS spread DS-CDMA is evaluated in a frequency- and time-selective Rayleigh fading channel. Also proposed is frequency-domain MAI-cancellation using decision feedback to improve the robustness against fast fading.

2. 2D-OVFS SPREADING AND CHIP INTERLEAVING

Uplink transmission model of DS-CDMA using 2D-OVFS spreading is illustrated in Fig.1, where only the u th user is shown (this scheme can also be applied to the DS-CDMA downlink transmission, however, this is not considered here).

A. Transmitted signal

The u th user's data-modulated symbol sequence $\{d_u(n); n=0 \sim (N_c/SF_f-1)\}$ is spread using the 1st OVSF spreading code $\{c_u^{SF_f}(t); t=0 \sim SF_f-1\}$ with spreading factor SF_f and further multiplied by a binary scramble sequence $\{c_u^{scr}(t); t=0 \sim N_c-1\}$ to produce a chip sequence of length of N_c chips (N_c is the FFT/IFFT block size for FDE). Next, the N_c -chip sequence is spread by the 2nd OVSF spreading code $\{c_u^{SF_t}(t); t=0 \sim SF_t-1\}$ with spreading factor SF_t . The 1st OVSF code is for multi-rate connection per user and the 2nd OVSF code is for orthogonal multiuser multiplexing.

As shown in Fig. 2, the overall spreading factor of 2D-OVSF codes is $SF = SF_t \times SF_f$, where SF_f can be arbitrarily selected independent of the FFT block size N_c , but $SF_f \leq N_c$ and SF_t is chosen according to the number of active users. If the number of users is U , then $SF_t = U$ can be used to allow U users access to the base station without causing the MAI.

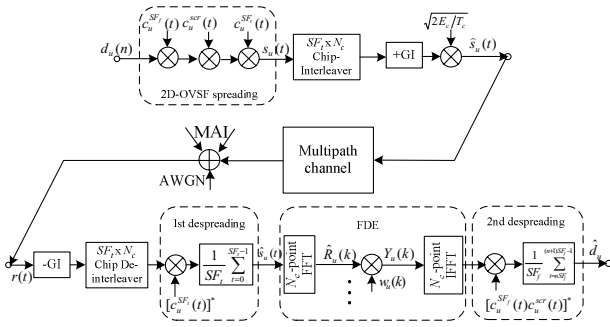


Fig. 1. Uplink transmission model for the u th user.

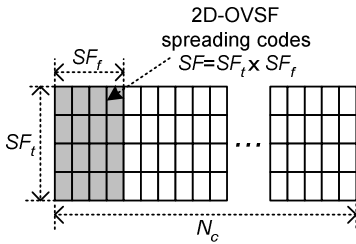


Fig. 2. 2D-OVSF spreading.

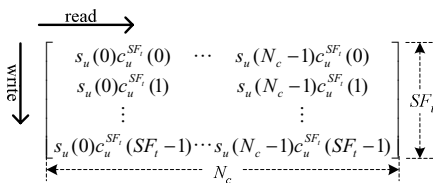


Fig. 3. Chip-interleaving.

After 2D-OVSF spreading, the chip interleaving is performed with column-wise input and row-wise output, as shown in Fig. 3. The 2D-OVSF spread DS-CDMA signal can be expressed using equivalent lowpass representation as

$$\hat{s}_u(t) = \sqrt{2E_c/T_c} s_u(t \bmod N_c) c_u^{SF_t}(\lfloor t/N_c \rfloor). \quad (1)$$

In Eq. (1), $s_u(t)$ is given by

$$s_u(t) = d_u(\lfloor t/SF_f \rfloor) c_u^{SF_f}(t \bmod SF_f) c_u^{scr}(t), \quad (2)$$

where $\lfloor x \rfloor$ is the largest integer smaller than or equal to x , E_c is the average chip energy and T_c is the chip duration of the 2nd OVSF spreading codes. An N_g -chip GI is inserted every N_c -chip block for FDE at a receiver.

B. Channel

The GI-inserted DS-CDMA signal is transmitted over a frequency- and time-selective Rayleigh fading channel. Assuming that the channel has L independent propagation paths, the discrete-time impulse response $h_u(t)$ of the u th user is expressed as

$$h_u(t) = \sum_{l=0}^{L-1} h_{u,l} \delta(t - \tau_{u,l}), \quad (3)$$

where $\delta(x)$ is the delta function and $h_{u,l}$ is the l th path gain with $\sum_{l=0}^{L-1} E[|h_{u,l}|^2] = 1$. Assuming block fading with the maximum Doppler frequency f_D , the path gains remain constant over one block interval $T = T_c(N_c + N_g)$ but vary block-by-block. The T_c -spaced distinct time delays are assumed to be $\{\tau_{u,l} = \tau_{u,l} + l; l=0 \sim L-1\}$ and $\tau_{u,l}$ is the u th user's transmit timing offset; the maximum time delay of each user's channel is shorter than GI.

C. Received signal

The sum of U users' faded signals is received by a base station receiver. The received signal is sampled at the chip rate and the GI is removed. The GI-removed received signal can be written as

$$r(t) = \sum_{u=0}^{U-1} h_u(t) \otimes \hat{s}_u(t) + n(t), \quad (4)$$

where \otimes denotes the convolution process and $n(t)$ is the additive white Gaussian noise (AWGN) with zero-mean and variance of $2N_0/T_c$ with N_0 being the one-sided power spectrum density.

D. MAI cancellation

$r(t)$ is deinterleaved (see Fig. 4) and then the 1st despreading is performed using the 2nd OVSF code $c_u^{SF_t}(t)$ as

$$\hat{s}_u(t) = \frac{1}{SF_t} \sum_{m=0}^{SF_t-1} r(t + mN_c) [c_u^{SF_t}(m)]^* \quad (5)$$

for $t=0 \sim N_c-1$. The MAI is cancelled due to the orthogonal property of OVSF spreading codes $\{c_u^{SF_t}(t); u=0 \sim U-1\}$. Hence, the multi-user channel is transformed into orthogonal single-user channels and the multiuser detection problem can be converted into a set of equivalent single-user equalization problems as in [15].

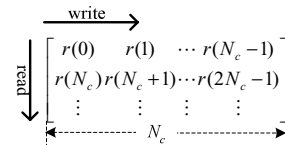


Fig. 4. Chip-deinterleaving.

After despreading, N_c -point fast Fourier transform (FFT) is applied to decompose the despread chip sequence $\{\hat{s}_u(t); t=0 \sim (N_c-1)\}$ into N_c frequency components $\{\hat{R}_u(k); k=0 \sim (N_c-1)\}$. $R_u(k)$ can be expressed as

$$\begin{aligned}\hat{R}_u(k) &= \frac{1}{\sqrt{N_c}} \sum_{t=0}^{N_c-1} \hat{s}_u(t) \exp(-j2\pi k \frac{t}{N_c}) \\ &= \sqrt{\frac{2E_c}{T_c}} S_u(k) H_u(k) + \Pi_u(k)\end{aligned}\quad (6)$$

where $S_u(k)$ is the k th frequency component of $s_u(t)$, $H_u(k)$ is the k th frequency channel gain of the u th user with $E[|H_u(k)|^2]=1$ and $\Pi_u(k)$ is the noise component due to the AWGN with zero-mean and variance of $2N_0/T_c$. Then, one-tap MMSE-FDE is carried out on each frequency component as

$$Y_u(k) = w_u(k) \hat{R}_u(k), \quad (7)$$

where $w_u(k)$ is the MMSE-FDE weight given by [7], [8]

$$w_u(k) = \frac{H_u^*(k)}{|H_u(k)|^2 + \left(SF_f \frac{E_c}{N_0}\right)^{-1}}. \quad (8)$$

Next, N_c -point inverse FFT (IFFT) is applied to $\{Y_u(k); k=0 \sim N_c-1\}$ to obtain the time-domain chip sequence:

$$y_u(t) = \frac{1}{\sqrt{N_c}} \sum_{k=0}^{N_c-1} Y_u(k) \exp(j2\pi k \frac{t}{N_c}). \quad (9)$$

Finally, the 2nd despreading using the 1st OVFSF spreading code $c_u^{SF_f}(t)$ is performed to get the decision variable $\hat{d}_u(n)$ for the detection of $d_u(n)$ as

$$\hat{d}_u(n) = \frac{1}{SF_f} \sum_{t=nSF_f}^{(n+1)SF_f-1} y_u(t) [c_u^{SF_f}(t) c_u^{scr}(t)]^*, \quad (10)$$

based on which data symbol decision is carried out.

3. FREQUENCY-DOMAIN MAI CANCELLATION

Time-domain MAI cancellation is based on the orthogonal property of the 2nd OVFSF codes $\{c_u^{SF_f}(t); u=0 \sim (U-1), t=0 \sim (SF_f-1)\}$. However, for channels with large Doppler spreads, the orthogonal property may be lost and the MAI is produced. To reduce the MAI for large Doppler spread, frequency-domain MAI cancellation is proposed below.

The k th frequency component $\hat{R}_u(k)$ in Eq. (6) can be rewritten as

$$\hat{R}_u(k) = \sqrt{2E_c/T_c} S_u(k) H_u(k) + M_u(k) + \Pi_u(k) \quad (11)$$

for $k=0 \sim (N_c-1)$, where $M_u(k)$ is the MAI component, given by

$$M_u(k) = \frac{1}{SF_f} \sqrt{\frac{2E_c}{T_c}} \sum_{\substack{u'=0 \\ u' \neq u}}^{U-1} S_{u'}(k) \sum_{m=0}^{SF_f-1} [c_{u'}^{SF_f}(m) c_u^{*SF_f}(m) H_{u',m}(k)], \quad (12)$$

where $H_{u',m}(k)$ is the k th subcarrier channel gain associated with the m th received chip block for the u' th user. The decision feedback is used to generate the replica of $S_{u'}(k)$ as

$$\tilde{S}_{u'}(k) = \frac{1}{\sqrt{N_c}} \sum_{t=0}^{N_c-1} \tilde{s}_{u'}(t) \exp(-j2\pi k \frac{t}{N_c}), \quad (13)$$

where $\tilde{s}_{u'}(t)$ is the replica of $s_{u'}(t)$, which is the spread and scrambled chip sequence represented by Eq. (2). The MAI component estimate $\tilde{M}_u(k)$ is obtained by replacing $S_{u'}(k)$ in Eq. (12) with $\tilde{S}_{u'}(k)$. As shown in Fig. 5, frequency-domain MAI-cancellation is performed as

$$\tilde{R}_u(k) = \hat{R}_u(k) - \tilde{M}_u(k). \quad (14)$$

Although the above frequency-domain MAI cancellation requires other users' channel state information and spreading codes to generate the MAI estimated $\tilde{M}_u(k)$, it is much simpler than MUD that requires the matrix inversion.

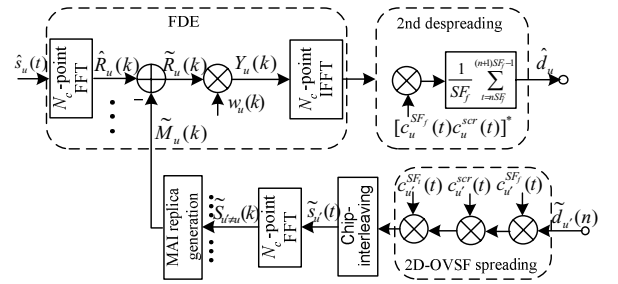


Fig. 5. Frequency-domain MAI-cancellation.

4. COMPUTER SIMULATION

We assume QPSK data-modulation, $N_c=256$ and $N_g=32$. An $L=16$ -path frequency-selective block Rayleigh fading channel having the uniform power delay profile is assumed. The transmit timing offsets $\{\tau_u\}$ are uniformly distributed over $[-\Delta/2, \Delta/2]$ with $\Delta < (N_g - L)$ and the maximum time delay difference is less than GI. Ideal channel estimation is assumed.

Fig. 6 plots the BER performance of uplink DS-CDMA as a function of the average received bit energy-to-the AWGN power spectrum density ratio E_b/N_0 , which is given by $E_b/N_0 = 0.5(E_c/N_0)(SF_f SF_f)(1 + N_g/N_c)$, for $U=1, 8$ and 16 when $f_D T = 10^{-6}$, where $T = SF_f \times SF_f \times T_c$ is the data symbol duration. The overall SF of 2D-OVSF spreading is $SF = SF_f \times SF_f = 16$ and we used $SF_f = U$ and $SF_f = 16/U$. For comparison, the BER performance of the conventional DS-CDMA using 1D-OVSF spreading is plotted in Fig. 6 for single-user detection (SUD) [16] and MUD [17] based on MMSE criterion. SUD cannot work for $U \geq 8$. When the system is moderately loaded, the MUD exhibits better performance; however, when

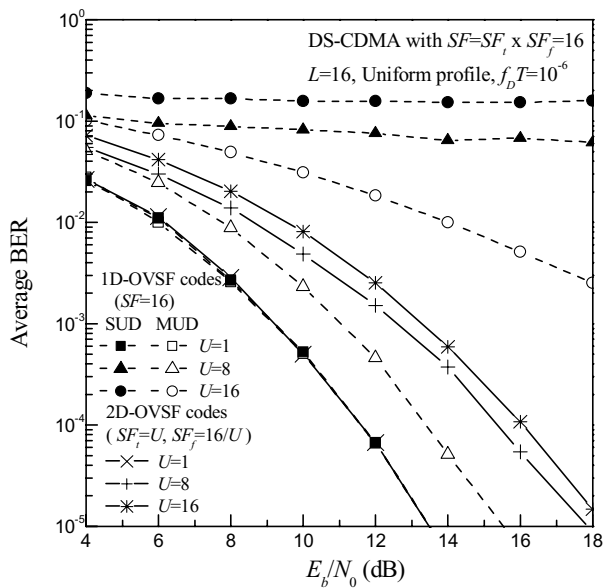


Fig. 6. BER performance comparison.

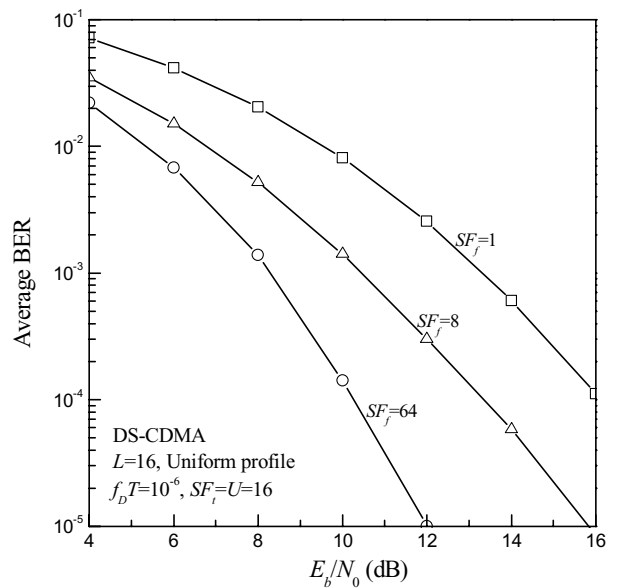


Fig. 7. BER performance of multi-rate full-loaded CI-DS-CDMA

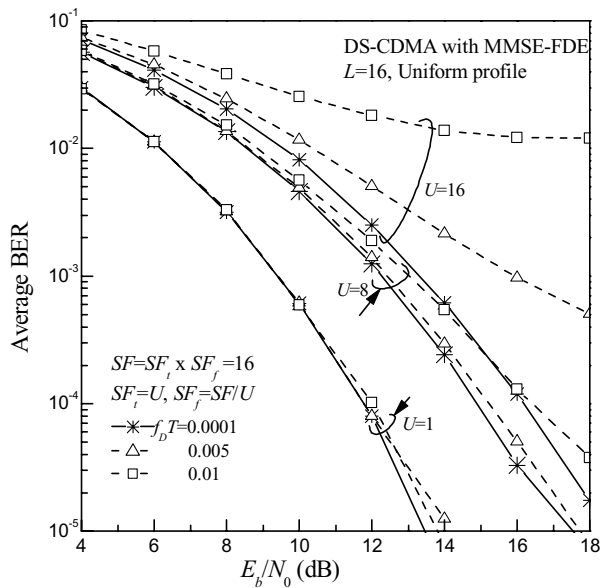


Fig. 8. Impact of $f_D T$.

the system is heavily loaded (i.e., $U \approx SF_i$), the BER performance degrades severely and our proposed 2D-OVSF spread DS-CDMA outperforms the MUD. MUD requires the knowledge of the spreading codes and multipath channels of all users and the computational complexity of MUD grows exponentially with the number of users; while the receiver complexity of 2D-OVSF spreading is linear. Hence, 2D-OVSF spreading is considered to be promising for the uplink transmission.

Fig. 7 shows the BER performance of full loaded 2D-OVSF spread DS-CDMA with $SF_i=U=16$. The overall spreading factor SF is $SF=16 \times SF_f$. The time-

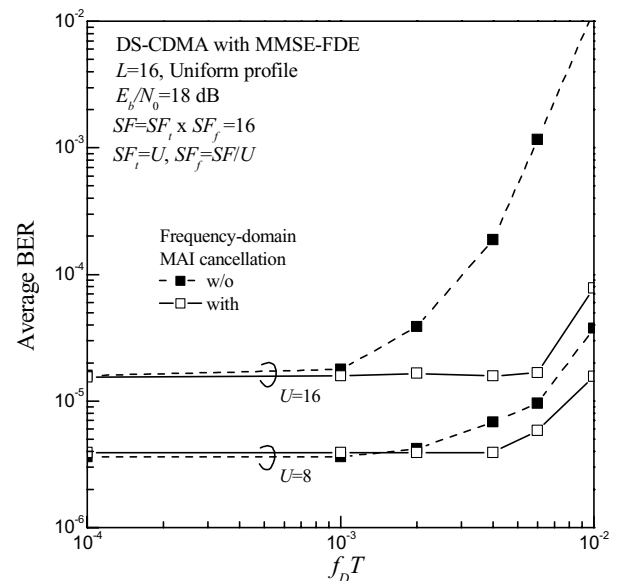


Fig. 9. Effect of frequency-domain MAI cancellation.

domain diversity is achieved by the despreading using the 2nd OVSF spreading code $c_u^{SF_f}(t)$ and the MAI is cancelled almost completely when $f_D T=10^{-6}$. The data symbol is spread over all frequencies using the 1st OVSF spreading code $c_u^{SF_i}(t)$, yielding large frequency diversity effect irrespective of SF_f . The reason for degrading performance with decreasing SF_f is due only to increasing self-chip interference (ICI) among chips of 1st OVSF spreading code [7].

Fig. 8 shows the impact of Doppler spread on the 2D-OVSF spread DS-CDMA for $SF=SF_i \times SF_f=16$, where

$SF_i=U$ and $SF_f=16/U$. Here, each user's signal is assumed to pass through independent fading channel but with the same $f_D T$. It is observed that the BER performance with $U=1$ remains almost the same if $f_D T$ is less than 0.01. However, the BER performance of the heavy-loaded case (i.e., $U=8$ and $U=16$) degrades severely for large $f_D T$ since the orthogonality among the 2nd OVFSF spreading codes cannot be maintained and hence the MAI appears. Therefore, the MAI cancellation technique is necessary to minimize the performance degradation caused by the orthogonality destruction of the 1st OVFSF spreading codes.

Fig. 9 plots the BER performance as a function of $f_D T$ for $U=8$ and 16 when $E_b/N_0=18$ dB. Our proposed frequency-domain MAI cancellation is very effective to improve the BER performance. The MAI cancellation effect is more significant as the number U of accessing users increases. For the full-loaded case ($U=16$), the BER performance can be almost the same until $f_D T$ approaches 8×10^{-3} (this corresponding to a mobile moving speed of 600 km/h at 5 GHz carrier frequency for 100 Mbps transmission).

5. CONCLUSIONS

In this paper, 2D-OVSF spreading was proposed to allow multi-rate transmission while mitigating the MAI for DS-CDMA uplink transmission. The use of 2D-OVSF spreading and chip interleaving can convert a multiuser detection (MUD) problem into a set of single-user equalization problems. 2D-OVSF spreading can not only increase the uplink capacity, but also has an a flexibility in providing multi-rate services. Computer simulation results have shown that the proposed 2D-OVSF spreading and decision feedback frequency-domain MAI-cancellation provides good BER performance in a multiuser frequency- and time-selective fading environment without using sophisticated MUD technique.

REFERENCES

- [1] F. Adachi, "Reverse link capacity of orthogonal multi-code DS-CDMA with multiple connections," IEICE Trans. Commun., vol. E85-B, no. 11, pp. 2522-2526, Nov. 2002.
- [2] A. J. Viterbi, CDMA: Principles of spread spectrum communications, Addison Wesley, 1995.
- [3] T. Ottosson and A. Svensson, "On schemes for multirate support in DS/CDMA," J. Wireless Personal Commun., vol. 6, no. 3, pp. 265-287, Mar. 1998.
- [4] F. Adachi, M. Sawahashi, and H. Suda, "Wideband DS-CDMA for next generation mobile communications systems," IEEE Commun. Mag., vol. 36, no. 9, pp. 56-69, Sep. 1998.
- [5] S. Hara and R. Prasad, "Overview of multicarrier CDMA," IEEE Commun. Mag., vol. 35, no. 12, pp. 126-144, Dec. 1997.
- [6] M. Helard, R. Le Gouable, J. -F. Helard, and J. -Y. Baudais, "Multicarrier CDMA techniques for future wideband wireless networks," Ann. Telecommun., vol. 56, pp. 260-274, 2001.
- [7] F. Adachi, D. Garg, S. Takaoka, and K. Takeda, "Broadband CDMA techniques," IEEE Wireless Commun. Mag., vol. 2, no. 2, pp. 2-13, Apr. 2005.
- [8] D. Falconer, S. L. Ariyavisitakul, A. Benyamin-Seeyar, and B. Eidson, "Frequency domain equalization for single-carrier broadband wireless systems," IEEE Commun. Mag., vol. 40, no. 4, pp. 58-66, April 2002.
- [9] G. B. Giannakis, Z. D. Wang, A. Scaglione and S. Barbarossa, "AMOUR-generalized multicarrier transceivers for blind CDMA regardless of multipath," IEEE Trans. Commun., vol. 50, no. 2, pp. 2064-2076, Feb. 2002.
- [10] H. Sari and G. Karam, "Orthogonal frequency-division multiple access and its applications to CATV network," Eur. Trans. Telecommun., pp. 507-516, Nov./Dec. 1998.
- [11] A. Stamoulis, Z. Q. Liu, and G. B. Giannakis, "Space-time block-coded OFDMA with linear precoding for multirate services," IEEE Trans. Signal Processing, vol. 50, no. 1, pp. 119-129, Jan. 2002.
- [12] Z. D. Wang and G. B. Giannakis, "Wireless multicarrier communications: Where Fourier meets Shannon," IEEE Signal Processing Mag., vol. 17, no. 3, pp. 29-48, May 2000.
- [13] Z. Wang and G. B. Giannakis, "Block precoding for MUI/ISI-resilient generalized multicarrier CDMA with multirate capabilities," IEEE Trans. Commun., vol. 49, no. 11, pp. 2016-2027, Nov. 2001.
- [14] S. Zhou, G. B. Giannakis and C. L. Martret, "Chip-interleaved block-spread code division multiple access," IEEE Trans. Commun., vol. 50, no. 2, pp. 235-248, Feb. 2002.
- [15] X. Peng, F. Chin, T. T. Tjhung and A. S. Madhukumar, "A simplified transceiver structure for cyclic extended CDMA system with frequency domain equalization," IEEE Proc. VTC'05 Spring, Sweden, pp. 1565-1569, May. 2005.
- [16] K. Ishihara, K. Takeda, and F. Adachi, "DS-CDMA frequency-domain multi-access interference canceller," IEICE Tech. Report, RCS2004-316, pp.155-160, Jan. 2005.
- [17] S. Tsumura, S. Hara, and Y. Hara, "Performance comparison of MC-CDMA and cyclically prefixed DS-CDMA in an uplink channel," IEEE Proc. VTC'04 Fall, Los Angeles, USA, pp. 414-418, Sept. 2004.